

Received 20 August 2022, accepted 13 September 2022, date of publication 16 September 2022, date of current version 27 September 2022.

Digital Object Identifier 10.1109/ACCESS.2022.3207546

RESEARCH ARTICLE

A Simple and Robust Model Predictive Current Control of PMSM Using Stator Current Predictor and Target-Oriented Cost Function

RONG FU 

School of Physics and Electrical Engineering, Weinan Normal University, Weinan 714099, China

e-mail: fr_wnu@163.com

This work was supported by the Talent Foundation of Weinan Normal University under Grant 17ZRRC03.

ABSTRACT Model predictive current control of permanent magnet synchronous motor(PMSM), which inherits from the vector control framework, has become a promising control strategy because of its simple structure and fast dynamic response. In order to protect the stator current prediction model from the influence of mismatched parameters, a simple and robust predictive current control with stator current predictor and target-oriented cost function (abbreviated as SCP-TOSF-PCC) is proposed in this paper. The feedback mechanism is introduced into the prediction equation in the discrete domain, and its design principle and stability analysis are also described in detail. In addition, different from the traditional cost function design method which is constructed by the tracking errors of stator current, this paper proposes a direct target-oriented cost function, which takes the average pulsations of d -axis current and q -axis current as the judge index. The design method of this cost function takes into account the influence of historical values on the voltage vector selection. The experimental results show that compared with the traditional methods, the proposed method has better dynamic, steady-state and robust performance.


INDEX TERMS Permanent magnet synchronous machine, model predictive control, predictive current control, robustness.

I. INTRODUCTION

Permanent magnet synchronous motor(PMSM) is widely used in electric vehicles, wind power generation and servo drive systems because of its high power density and excellent control performance. Finite control set-model predictive control(FCS-MPC) was first proposed by Jose Rodriguez, a Chilean scholar, in 2004, because of its intuitive concept, fast dynamic response and easy multi-objective optimization, and is widely used in the field of power electronics and electrical drive [1], [2], [3], [4], [5], [6]. Model predictive current control (MPCC) strategy of permanent magnet synchronous motor, which retains the basic principle of vector control, is considered to be a promising method. In [7], for the PMSM drive system of electric vehicle, the author compares the vector control and predictive current control strategies

in detail. The experimental results show that predictive current control has faster dynamic performance, smaller stator current harmonics (at the same switching frequency), smaller electromagnetic torque ripple and electromagnetic interference performance.

For predictive current control of PMSM, mismatched motor parameters will lead to stator current prediction errors and reduce the control performance of the system [8], [9]. Scholars mainly improve the prediction accuracy of stator current from two aspects. One method is to propose deadbeat predictive current control (DPCC) based on the disturbance observer. The voltage vector reference is calculated based on the deadbeat principle. The voltage vector calculation error caused by mismatch parameters is regarded as a disturbance, and the error is estimated and compensated in realtime based on the disturbance observer. In [10], static-errorless deadbeat predictive current control using a second-order sliding-mode disturbance observer is proposed to avoid to suffer from

The associate editor coordinating the review of this manuscript and approving it for publication was Fangfei Li .

problems of steady state current error and stability. In [11], for PMSM drives, DPCC with model mismatch is firstly analyzed and then a stator current and disturbance observer based on sliding-mode exponential reaching law is proposed to suppress model parameter mismatch and one-step control delay. In [12], a moving horizon estimator is proposed to estimate the back-electromotive force and the disturbance caused by parameter variations. However, another method is to introduce the online parameter identification theory into the predictive current control, and update the predictive model in realtime to realize the accurate prediction of stator current vector. In [13], for stator resistance and inductance of PMSM DPCC, a novel parameters identification based on reconstructed characteristic vector from the disturbance observer is developed to update the model parameters. In [14], the white-box model of PMSM is developed firstly for DPCC, and then data-driven recursive least squares estimation is proposed to observe the parameters of white-box model. Therefore, establishing a simple and robust stator current predictor has always been the research goal of community of scholars.

In model predictive control, the cost function is utilized to select the optimal voltage vector. The cost function usually includes electromagnetic torque tracking, stator flux tracking, switching frequency limitation and over-current protection. Among them, each item should have different dimensions, so the weighting factors are needed to weigh the importance of each item. Due to the lack of theoretical guidance, the cut-and-trial method is often used to set the weight factors, which is cumbersome and can not obtain the optimal solution. Scholars have put forward many solutions to this problem. One method is to decompose the multi-objective optimization problem into multiple single objective optimization problems. In [15], tolerant sequential model predictive control is proposed to solve a multi-objective optimization problem. The voltage vectors satisfying the torque tolerance are firstly selected, and then the optimal vector is selected by minimizing the flux cost function. In [16], two cost functions, the one for the electromagnetic torque tracking and other for the stator flux magnitude, are designed to select two sets of voltage vectors, respectively. Then, the optimal vector is selected from two sets of vectors, using the predefined algorithm. Another scheme is to convert the cost function into stator flux vector reference based on the relationship between the electromagnetic torque reference and stator flux amplitude reference, so the weight factor is cancelled. In [17], model predictive flux control of induction machine drives are firstly developed. The calculation method converting torque and flux magnitude into stator flux vector is presented in detail. This method not only cancels the weight factor, but also has excellent control performances. In [18], model predictive flux control for PMSM drives is developed, and then the robustness is analysed and the compensated strategy based on sliding mode observer is utilized to improve the robustness. In recent years, scholars have introduced neural networks, intelligent optimization algorithms and other theories into

the setting of weight factors. In [19], artificial neural networks(ANN) are trained by simulation data or experimental data through the fitness function, and then ANN are utilized to design the weighing factors for different states of induction machine. In [20], online weighting factor optimization by simplified simulated annealing for induction machine drives are proposed, where during every control period, the weighing factor is optimized by intelligent algorithm. This strategy ensures the optimal factor for every control period, and the limitation of the maximum iteration step prevents the algorithm from falling into a dead loop. In [21], for predictive current controller of a six-phase induction machine, a weighting factor design based on particle swarm optimization algorithm is proposed to coordinated torque currents and harmonic currents. It is known that the introduction of intelligent optimization algorithm provides a better solution to set the weight factors, but it also increases the complexity of the system. In addition to the cost function, the implementation of intelligent optimization algorithm introduces the fitness function. Therefore, the simple and effective setting methods of weight factors has always been the goal of academia.

Aiming at the two problems of robustness and weight factor design method of predictive current control, this paper proposes robust stator current predictor and target-oriented cost function design methods, respectively. The arrangement of this paper is as follows: Section II introduces the traditional predictive current control, and then analyzes the robustness of stator current predictive equation under mismatched parameters. In Section III, the design method and stability analysis of robust stator current predictor are described in detail. Section III also expounds the design principle of target-oriented cost function. Section IV verifies the effectiveness of the proposed algorithm through experiments. Finally, this paper is summarized in Section V.

II. MATHEMATICAL MODEL OF PMSM AND T-PCC

A. MATHEMATICAL MODEL OF PMSM

In stator reference frame, based on the space vector theory, the mathematical equations of PMSM are presented in (1)-(3), where v_s , i_s and ψ_s are stator voltage vector, stator current vector and stator flux vector, respectively. R_s , L_s and ψ_f are stator resistance, excitation inductance and permanent magnet flux, respectively. The voltage vector v_s can be generated by two-lever voltage source inverter.

$$v_s = R_s i_s + \frac{d\psi_s}{dt} \quad (1)$$

$$\psi_s = L_s i_s + \psi_f e^{j\theta_r} \quad (2)$$

$$v_s = R_s i_s + L_s \frac{di_s}{dt} + j\omega_r \psi_f e^{j\theta_r} \quad (3)$$

Stator current equation (3) can be converted into the rotor magnetic field frame system, which is expressed as (4). v_{dq_s} and i_{dq_s} are the vectors in the rotor magnetic field frame system. Transformation equation for i_s and i_{dq_s} is as follows:

$i_{dqs} = i_s e^{-j\theta_r}$, where θ_r is the rotor position of PMSM [22].

$$v_{dqs} = R_s i_{dqs} + L_s \frac{di_{dqs}}{dt} + jL_s \omega_r i_{dqs} + j\omega_r \psi_f \quad (4)$$

B. TRADITIONAL PREDICTIVE CURRENT CONTROL

In the model predictive current control, according to the stator current equation (3) and the first-order Euler discretization equation (5), the predictive equation of stator current can be expressed as equation (6).

$$y_{n+1} = y_n + hf(y_n, x_n) \quad (5)$$

$$i_s(k+1) = i_s(k) + \frac{T_s}{L_s}(v_s(k) - R_s i_s(k)) - \frac{T_s}{L_s} j\omega_r \psi_f e^{j\theta_r(k)} \quad (6)$$

The cost function for predictive current control is designed as (7), where $i_s^*(k+1)$ denotes the stator current reference.

$$g_j = |i_s^*(k+1) - i_s(k+1)_j| \quad (7)$$

The block diagram of traditional predictive current control (T-PCC) is illustrated in Fig.1. In the digital control system, the implementation process of T-PCC is mainly divided into the following steps:

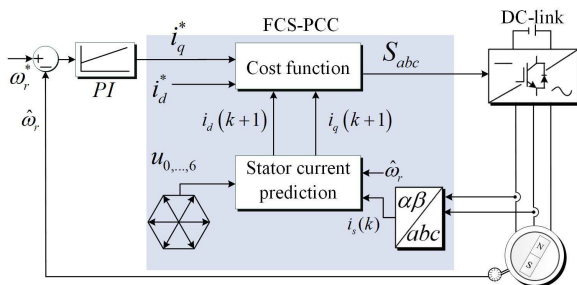


FIGURE 1. Diagram of traditional model predictive current control.

Step I: measure the stator currents i_a, i_b , and obtain the stator current vector i_s at the sampling time k by Clarke transform.

Step II: based on the stator current prediction equation (6), calculate the stator current vectors $i_s(k+1)_j$ at the sampling time $k+1$ for seven different voltage vectors.

Step III: based on the cost function (7), the voltage vector that minimizes the cost function is selected as the optimal one, and applied at the sampling time $k+1$.

C. ROBUSTNESS ANALYSIS OF MISMATCHED PARAMETERS

During the operation of PMSM, the winding temperature rise will lead to the increase of stator resistance R_s . The over saturation of magnetic circuit will lead to the decrease of excitation inductance L_s , and the eddy current loss of permanent magnet will lead to the temperature rise of permanent magnet, which will lead to the decrease of permanent magnet flux linkage ψ_f . According to the prediction equation (6),

the mismatched PMSM parameters will lead to the prediction errors of stator current vector.

In order to analyze the influence of mismatched parameters on the prediction errors of stator current vector, a detailed analysis in theory is presented in this paper. The nominal parameters of PMSM are set as R_s, L_s and ψ_f , and the corresponding prediction equation is the equation (6). The mismatch parameters of PMSM are set as \tilde{R}_s, \tilde{L}_s and $\tilde{\psi}_f$, and the corresponding prediction equation is expressed as (8).

$$\tilde{i}_s(k+1) = i_s(k) + \frac{T_s}{\tilde{L}_s}(v_s(k) - \tilde{R}_s i_s(k)) - \frac{T_s}{\tilde{L}_s} j\omega_r \tilde{\psi}_f e^{j\theta_r(k)} \quad (8)$$

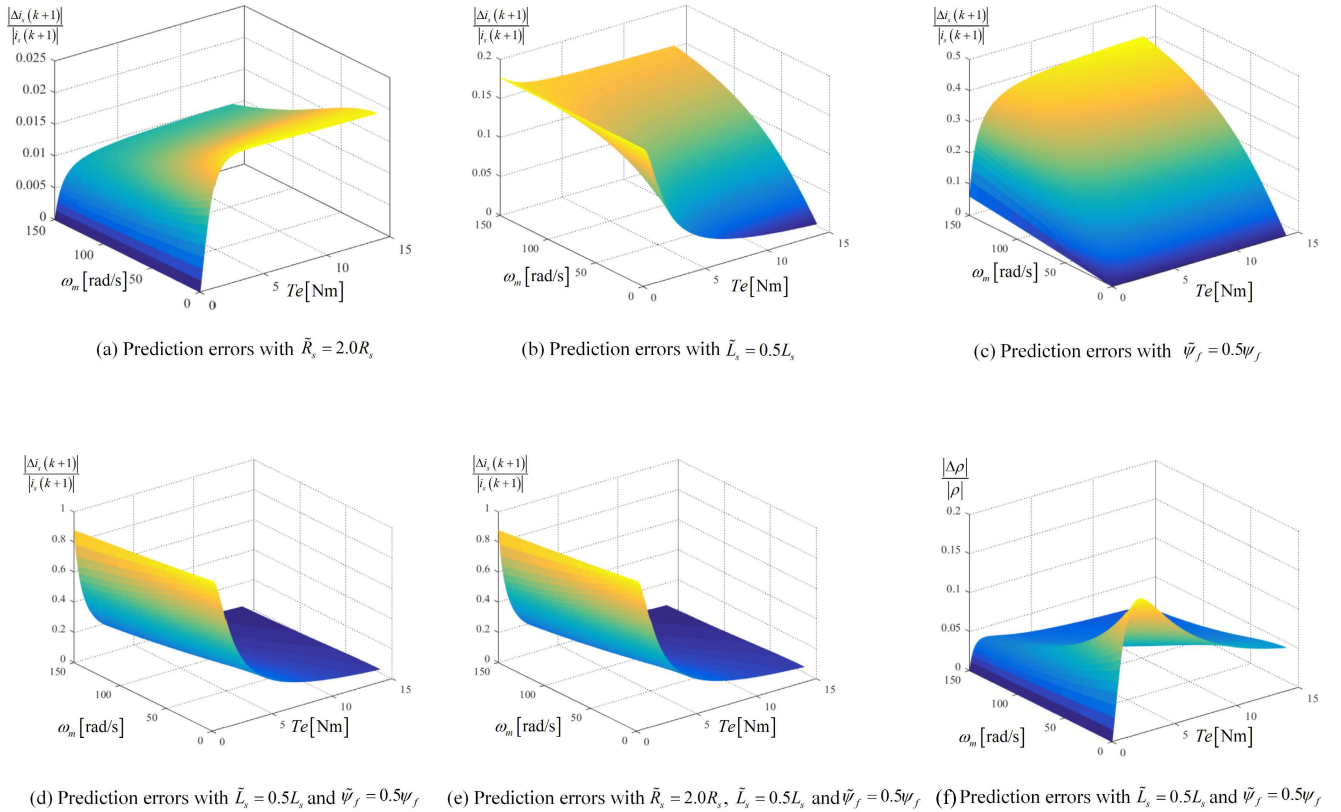
The stator current prediction error is defined as $\frac{|\Delta i_s(k+1)|}{|i_s(k+1)|}$, where $\Delta i_s(k+1)$ the difference between $\tilde{i}_s(k+1)$ and $i_s(k+1)$, that is, $\Delta i_s(k+1) = \tilde{i}_s(k+1) - i_s(k+1)$. The angle prediction error of stator current vector is defined as $\frac{|\Delta \rho|}{|\rho|}$, where $\rho = \angle i_s$ and $\Delta \rho = \angle \tilde{i}_s - \angle i_s$. When $\tilde{R}_s = 2.0R_s$, the prediction error of stator current vector is presented in Fig.2(a). It can be seen that, from Fig.2(a), The stator current error $\frac{|\Delta i_s(k+1)|}{|i_s(k+1)|}$ increases with the increase of electromagnetic torque, while $\frac{|\Delta i_s(k+1)|}{|i_s(k+1)|}$ decreases with the increase of the rotor speed. The maximum value of stator current error is 0.019, i.e. 1.9%. In Fig.2(b), the prediction error increases with the increase of rotor speed, while the electromagnetic torque has little effect on it, but the electromagnetic torque has a greater effect only under light-load state. Under high-speed and light-load states, the maximum value of $\frac{|\Delta i_s(k+1)|}{|i_s(k+1)|}$ is 17.5%. In Fig.2(c), $\frac{|\Delta i_s(k+1)|}{|i_s(k+1)|}$ is directly proportional to the speed and torque, and the maximum value of it is 41.2%. When $\tilde{L}_s = 0.5L_s$ and $\tilde{\psi}_f = 0.5\psi_f$, stator current prediction error is more serious due to the combined action of mismatched inductance and permanent magnet flux, which is illustrated in Fig.2(d). For $\tilde{R}_s = 2.0R_s, \tilde{L}_s = 0.5L_s$ and $\tilde{\psi}_f = 0.5\psi_f$, there is little difference between Fig.2(d) and Fig.2(e). Therefore, it can be concluded that the influence of mismatched stator resistance is very small compared with \tilde{L}_s and $\tilde{\psi}_f$. Fig.2(e) presents the angle prediction error of stator current vector, and its maximum value is 19.3%.

From the above analysis, it can be seen that the mismatched stator resistance has little impact on the stator current prediction error, while the mismatched excitation inductance and permanent magnet flux linkage have a great impact on the stator current prediction error. The mismatched parameters have little effect on the angle prediction error. The stator current prediction error is related to electromagnetic torque, speed, rotor position and voltage vector, and its variation law is complex.

III. STATOR CURRENT PREDICTOR AND TARGETED-ORIENTED COST FUNCTION

A. DESIGN OF STATOR CURRENT PREDICTOR

For stator current prediction errors caused by mismatched parameters, stator current predictor is developed, where


FIGURE 2. Analysis of stator current prediction errors for mismatched parameters.

a simple feedback mechanism is utilized to compensate for prediction errors. It is known that stator current equation (3) can be rewritten as (9).

$$L_s \frac{di_{dqs}}{dt} = v_{dqs} - R_s i_{dqs} - jL_s \omega_r i_{dqs} - j\omega_r \psi_f \quad (9)$$

Correspondingly, the complex domain expression of stator current equation (9) is expressed in (10), where $v_{dqs}(s)$ and $i_{dqs}(s)$ are the Laplace transforms of v_{dqs} and i_{dqs} in time domain.

$$i_{dqs}(s) = \frac{1}{R_s} \left(\frac{1}{\frac{L_s}{R_s}s + 1} \right) [v_{dqs}(s) - j\omega_r (L_s i_{dqs}(s) + \psi_f)] \quad (10)$$

The step response method is utilized to achieve the discrete mathematical equations, and the feedback compensation mode is proposed to eliminate the prediction error. And then, the stator current predictor is developed, which is expressed as (11). $v_{sum}(k+1)$ represents the total compensation item, which is mainly composed of two parts. one is the cross coupling part, that is, $\omega_r L_q i_{qs}(k+1) - j\omega_r L_d i_{ds}(k+1) - j\omega_r \psi_f$, the other is current compensation, $(k_1 + T_s k_2) i_{s_error}(k+1) + k_1 i_{s_error}(k)$. The block diagram of stator current predictor is shown in Fig.3, where $\tau = L_s / R_s$.

$$i_{dqs}(k+2) = i_{dqs}(k+1) e^{-\frac{T_s}{\tau}}$$

$$v_{sum}(k+1) = v_{sum}(k) + (k_1 + T_s k_2) i_{s_error}(k+1) + k_1 i_{s_error}(k) + v_{dqs}(k+1) + \omega_r L_q i_{qs}(k+1) - j\omega_r L_d i_{ds}(k+1) - j\omega_r \psi_f \quad (11)$$

It is known that at k sampling instant, stator current $i_s(k+1)$ cannot be measured, and only the actual stator current $i_s(k)$ can be measured by stator current sensor. The actual stator current $i_s(k+1)$ is estimated by Langrange extrapolation method (13) in this paper. And then, the prediction error of stator current at $k+1$ sampling instant can be computed by the equation (14).

$$i_{dqs}(k+1) = \sum_{l=0}^n (-1)^{n-l} \binom{n+1}{l} i_{dqs}(k+l-n) \quad (13)$$

$$i_{dqs_error}(k+1) = i_{dqs}(k+1) - \hat{i}_{dqs}(k+1) \quad (14)$$

According to the control theory of linear discrete system, the transfer function of stator current predictor can be expressed as (15),

$$\frac{i_{dqs}(k+2)}{i_{dqs}(k+1)} = \frac{M_1 z + M_2}{E_1 z^2 + E_2 z + E_3} \quad (15)$$

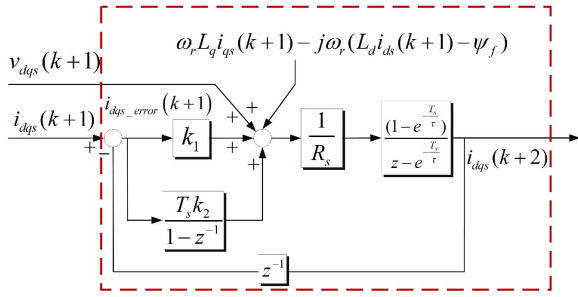


FIGURE 3. Diagram of stator current prediction based on closed-loop model.

where M_1, M_2, E_1, E_2 and E_3 are presented as follows:

$$M_1 = -k_1 + k_1 e^{-\frac{T_s}{\tau}} - k_2 T_s + k_2 T_s e^{-\frac{T_s}{\tau}}$$

$$M_2 = -k_1 e^{-\frac{T_s}{\tau}}$$

$$E_1 = -R_s$$

$$E_2 = R_s \left(1 + e^{-\frac{T_s}{\tau}}\right) - k_1 \left(1 - e^{-\frac{T_s}{\tau}}\right) - k_2 T_s \left(1 - e^{-\frac{T_s}{\tau}}\right)$$

$$E_3 = -R_s e^{-\frac{T_s}{\tau}} + k_1 \left(1 - e^{-\frac{T_s}{\tau}}\right)$$

The closed-loop pole distribution of stator current predictor for different values of k_1 and k_2 is illustrated in Fig.4. Based on the control theory of linear discrete system, the poles should be distributed in the right-half plane of the unit circle and close to the origin as far as possible, so that the system can have better dynamic performance. However, in the actual system, the distribution of poles can not be very close to the origin, so as to prevent the disturbance from causing the poles to be distributed in the left-half plane. Therefore, in this paper, the values of parameters are as follows: $k_1 = 4.0$; $k_2 = \frac{5.0}{T_s}$.

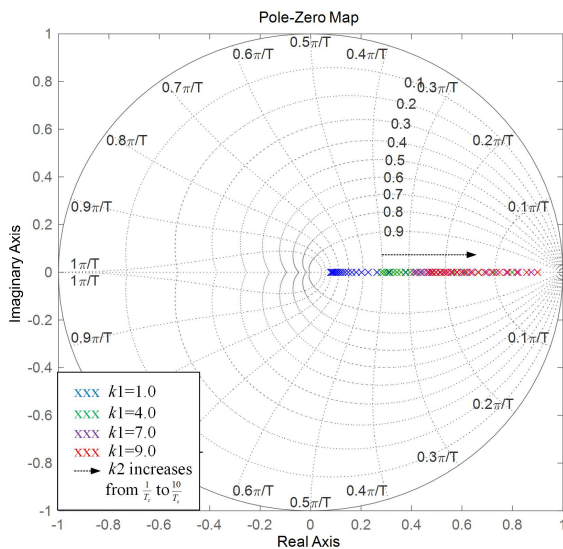


FIGURE 4. The closed-loop pole distribution of stator current predictor.

B. TARGETED-ORIENTED COST FUNCTION

In model predictive current control of PMSM, the cost function is usually designed as equation (16) or equation (17),

where the equation (16) is the cost function in stator reference frame system and equation (17) is the cost function in dq -axis (17) system. In (16), λ_β is the weight factor. Because i_α and i_β belong to the same dimension, it is usually set as $\lambda_\beta = 1$ for simplicity. However, $\lambda_\beta = 1$ is not the optimal value, which has been studied in detail in [23].

$$g_j = |i_\alpha^* - i_\alpha(k+2)| - \lambda_\beta |i_\beta^* - i_\beta(k+2)| \quad (16)$$

$$g_j = |i_d^* - i_d(k+2)| - \lambda_q |i_q^* - i_q(k+2)| \quad (17)$$

The above cost functions only are designed by stator current error at $k+2$ sampling instant, and does not consider stator current errors at the past sampling instants (i.e. sampling instant $k+1, k, k-1$, etc.). It is known that, in essence, the cost function is utilized to select the optimal voltage vector to achieve the minimum stator current ripple and the fastest dynamic response.

In this paper, the target-oriented cost function is proposed for the first time, which directly takes the stator current ripple as the evaluation index and cancels the setting of weight factor. For d -axis stator current, the current ripple $RMSE_{dj}$ is defined as (18), where N represents the calculated number of stator current $i_{dj}(k+2-i)$. In this paper, $N = 9$, which means that $i_d(k+2), \dots, i_d(k-7)$ are involved in the calculation of d -axis stator current ripple. Similarly, the current ripple $RMSE_{qj}$ is defined as (19).

$$RMSE_{dj} = \sqrt{\frac{1}{N+1} \sum_{i=0}^N |i_d^*(k+2-i) - i_{dj}(k+2-i)|^2} \quad (18)$$

$$RMSE_{qj} = \sqrt{\frac{1}{N+1} \sum_{i=0}^N |i_q^*(k+2-i) - i_{qj}(k+2-i)|^2} \quad (19)$$

Therefore, the stator current vector ripple is defined as equation (20), and the targeted-oriented cost function is designed as equation (21).

$$RMSE_{daj} = \sqrt{RMSE_{dj}^2 + RMSE_{qj}^2} \quad (20)$$

$$g_j = RMSE_{daj} |_{j=1, \dots, 7} \quad (21)$$

C. OVERALL BLOCK DIAGRAM OF THE PROPOSED ALGORITHM

The block and flow diagrams of the proposed algorithm are illustrated in Fig.5 and Fig.6. The implementation process of the proposed algorithm is mainly divided into the following steps:

Step I: measure stator current $i_s(k)$ and rotor speed ω_r .

Step II: Based on $i_{dqs}(k), v_{opt}(k)$ and stator current predictor, stator current $i_{dqs}(k+1)$ at k sample instant are estimated, in order to eliminate the delay of the digital system, where $v_{opt}(k)$ is the optimal vector computed at last sampling period.

Step III: For seven different voltage vectors, stator current $i_{dqs}(k+2)$ is predicted by the proposed stator current predictor.

Step IV: Stator current ripples are computed for seven different vectors by the equations (18)-(21).

Step V: The optimal voltage vector $v_{opt}(k+1)$ is obtained by targeted-oriented cost function (21), and applied at $k+1$ sample instant.

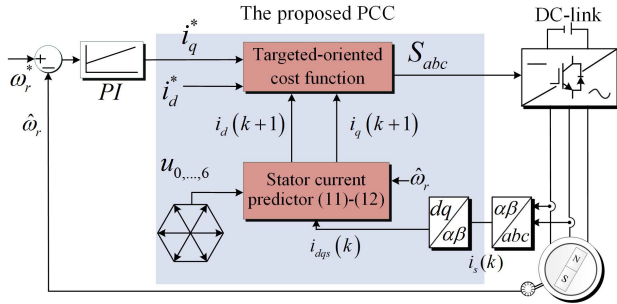


FIGURE 5. Diagram of the proposed predictive current control.

IV. EXPERIMENTAL VERIFICATION

A. EXPERIMENTAL PLATFORM

The traditional PCC (T-PCC) and proposed SCP-TOSF-PCC are verified at the experimental platform of PMSM drives, which is illustrated in Fig.7. The PMSM (C) is driven by IGBT-based voltage source inverter (B) and controlled by digital signal processor (TMS320F28335). The algorithms of T-PCC and SCP-TOSF-PCC are programmed and executed in digital signal processor. The experimental results are obtained by the oscilloscope (E) and are drawn in MATLAB. The parameters of PMSM are illustrated in Table 1.

TABLE 1. Parameters of PMSM.

Descriptions	Parameters	Nominal Values
DC-link Voltage	V_{dc} [V]	520
Rated Power	P_N [kW]	2.1
Rated Voltage	U_N [V]	304
Rated Speed	ω_{nom} [r/min]	1500
Rated Torque	T_e [Nm]	13.2
Number of Pole Pairs	p	4.0
Stator Resistance	R_s [Ω]	2.826
Stator Inductance	L_s [mH]	14.69
PM Flux	ψ_f [Wb]	0.321

The dynamic performances of the proposed SCP-TOSF-PCC are presented in Fig.8. From up to down, the rotor speed n , the electromagnetic torque T_e , the stator flux magnitude $|\psi_s|$ and stator current i_d are presented in Fig.8. The commands of speed are set as 800 rpm at 0.0 s, 500 rpm at 2.0 s, 1500 rpm at 4.0 s and 800 rpm at 6.0 s. The load torque is set as 5.0 N · m. Fig.8 shows that the proposed SCP-TOSF-PCC has excellent dynamic performance.

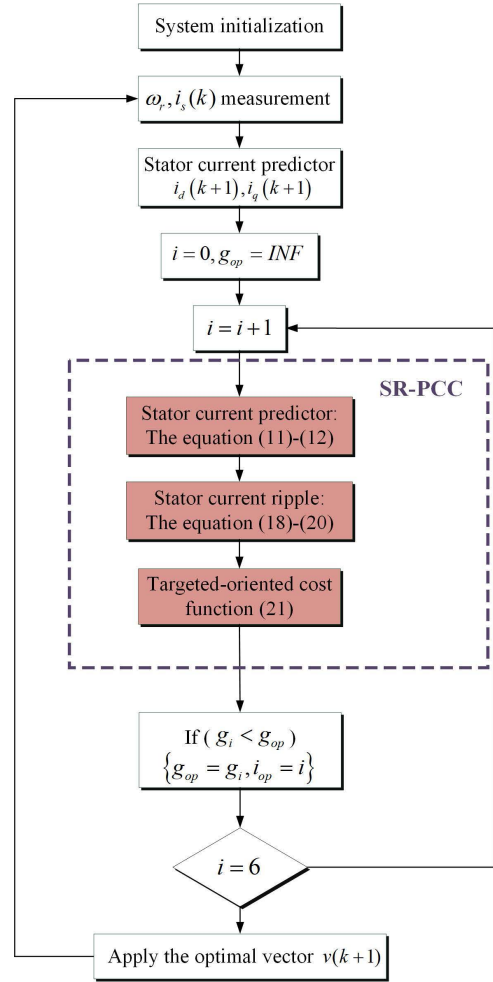


FIGURE 6. Flow diagram of the proposed predictive current control.

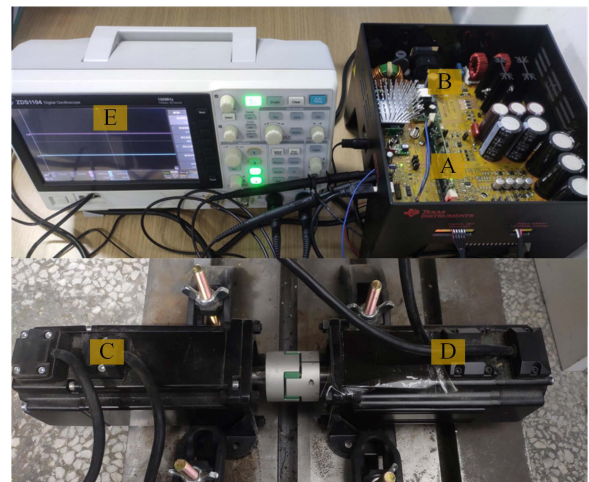


FIGURE 7. The experimental platform of PMSM, (A) TMS320F28335, (B) voltage source inverter, (C) PMSM, (D) the load motor, (E) oscilloscope.

The response time is 0.1 s from 500 rpm to 1500 rpm at 4.0 s. Correspondingly, the response time of the electromagnetic torque is 2.5 ms. The THD (Total Harmonic Distortion) of stator current is 11.32%.

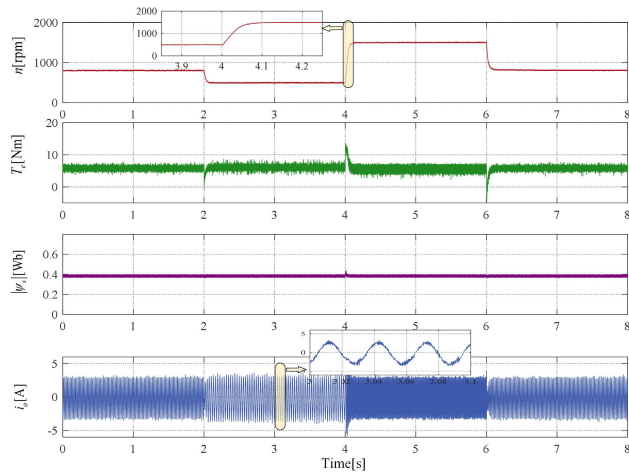


FIGURE 8. The dynamic-state performances of the proposed SCP-TOSF-PCC for PMSM drives.

The dynamic response time of SCP-TOSF-PCC is 0.1 s, while that of T-PCC is 0.13 s. It can be seen that the dynamic performance of SCP-TOSF-PCC is slightly faster than that of T-PCC. There are two main reasons for this result. One is that SCP-TOSF-PCC and T-PCC adopt the same PI speed regulator in the speed loop, and the regulation performance of the speed loop is mainly determined by the speed controller. Secondly, the main function of the proposed SCP-TOSF-PCC algorithm is to improve the robustness of the control system and reduce the torque ripple and the total harmonic distortion of the stator current.

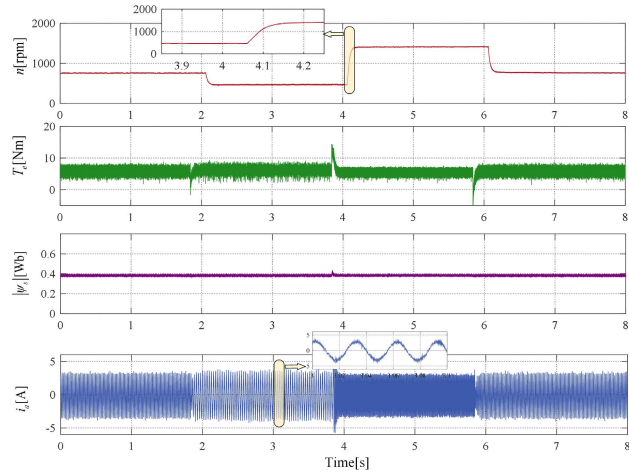


FIGURE 9. The dynamic-state performances of the T-PCC for PMSM drives.

The steady-state performances of the proposed SCP-TOSF-PCC are presented in Fig.10. It is known that the proposed algorithm also has excellent performances. The ripple of electromagnetic torque T_e is only $2.1 N \cdot m$. The THD of stator current is 11.67%.

In the actual operation of PMSM drives, the sudden change of load torque often occurs. The dynamic performances with

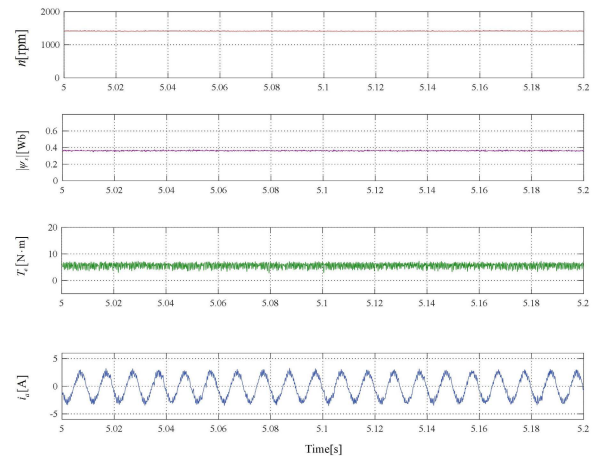


FIGURE 10. The steady-state performances of the proposed SCP-TOSF-PCC for PMSM drives.

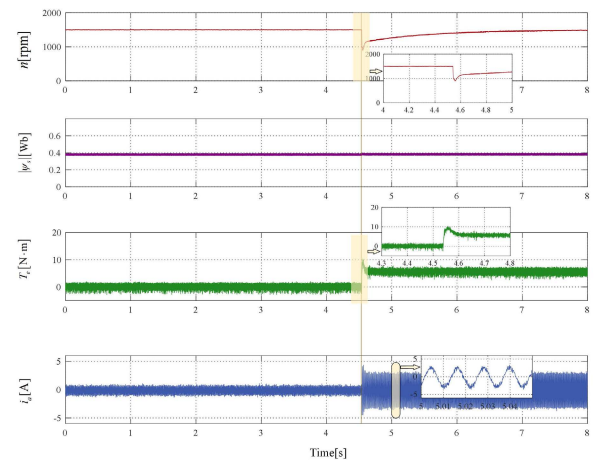


FIGURE 11. The speed recovery performances with load torque occurring suddenly of the proposed SCP-TOSF-PCC for PMSM drives.

load torque occurring suddenly for the proposed SCP-TOSF-PCC are illustrated in Fig.11. From Fig.11, it can be seen that the proposed SCP-TOSF-PCC has excellent speed recovery ability. The load torque $5.5 N \cdot m$ is exerted at 4.54 s, and the electromagnetic torque immediately becomes $5.5 N \cdot m$.

The robustness experiments of T-PCC and SCP-TOSF-PCC are illustrated in Fig.12 and Fig.13. The robustness test method is to use mismatched motor parameters in the control algorithms executed by DSP controller. In 0-4.0 s, the T-PCC algorithm is executed in DSP controller, and in 4.0-8.0 s, the proposed SCP-TOSF-PCC algorithm is executed in DSP controller. For $L_s^* = 2.0L_s$, where L_s^* denotes the mismatched parameter and L_s is nominal parameter, the experimental result is presented in Fig.12. It can be seen that the proposed SCP-TOSF-PCC has better robustness than the traditional T-PCC. For T-PCC of PMSM, the ripple of stator flux magnitude is 0.025 Wb and that of SCP-TOSF-PCC is only 0.015 Wb. The ripple of electromagnetic torque for the proposed SCP-TOSF-PCC is $2.5 N \cdot m$, which is 28.6% lower than that of T-PCC.

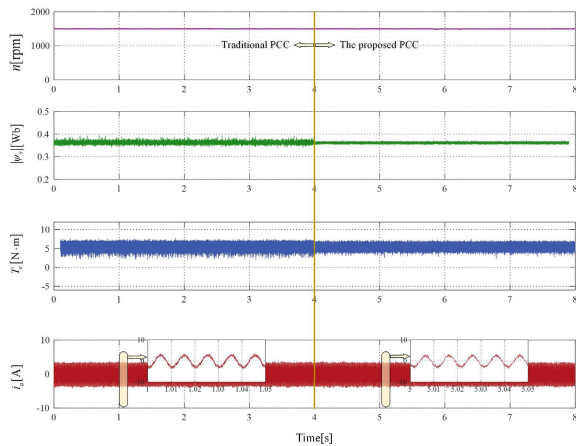


FIGURE 12. The robustness performances of T-PCC and the proposed SCP-TOSF-PCC with $L_s^* = 2.0L_s$.

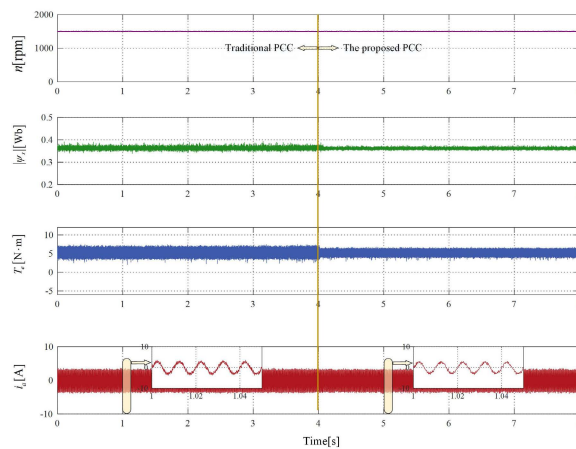


FIGURE 13. The robustness performances of T-PCC and the proposed SCP-TOSF-PCC with $\psi_f^* = 0.5\psi_f$.

For $\psi_f^* = 0.5\psi_f$, Fig.13 shows the results of experiments. ψ_f^* denotes the mismatched parameter, which is used in predictive controller, and ψ_f represents the permanent magnet flux linkage parameter of permanent magnet synchronous motor itself. According to the formula $T_e = 1.5p\psi_f i_q$, for T-PCC and SCP-TOSF-PCC, in steady state, stator currents of T-PCC and SCP-TOSF-PCC have the equal amplitudes. Because the proposed stator current predictor can offset the prediction error caused by mismatched permanent magnet flux by using the compensation term, the proposed SCP-TOSF-PCC has smaller electromagnetic torque ripple, stator flux amplitude ripple and THD of stator current. The THD of stator current for the proposed SCP-TOSF-PCC is 11.83%, which is 22.7% lower than that of T-PCC.

V. CONCLUSION

Aiming at the problem that the current prediction model depends on motor parameters and the cost function design only considers the current sampling time, the SCP-TOSF-PCC control algorithm is proposed in this paper.

Compared with the traditional open-loop prediction model, the stator current predictor proposed in this paper can overcome the prediction error caused by mismatch parameters by introducing a simple feedback mechanism. For the design of cost function, this paper proposes a targeted-oriented cost function design method, which directly takes the ripple of d -axis stator current and q -axis stator current as the evaluation index, which has the advantages of simplicity and directness. Experimental results show that the proposed algorithm has excellent dynamic performance, steady-state performance and speed recovery performance. For the mismatched parameters, the proposed SCP-TOSF-PCC algorithm has better robustness than the traditional methods.

REFERENCES

- [1] S. Vazquez, J. Rodriguez, M. Rivera, L. G. Franquelo, and M. Norambuena, "Model predictive control for power converters and drives: Advances and trends," *IEEE Trans. Ind. Electron.*, vol. 64, no. 2, pp. 935–947, Nov. 2017.
- [2] M. Preindl and S. Bolognani, "Model predictive direct speed control with finite control set of PMSM drive systems," *IEEE Trans. Power Electron.*, vol. 28, no. 2, pp. 1007–1015, Feb. 2013.
- [3] V. Yaramasu, B. Wu, S. Alepuz, and S. Kouro, "Predictive control for low-voltage ride-through enhancement of three-level-boost and NPC-converter-based PMSG wind turbine," *IEEE Trans. Ind. Electron.*, vol. 61, no. 12, pp. 6832–6843, Dec. 2014.
- [4] X. Ding, M. Du, C. Duan, H. Guo, R. Xiong, J. Xu, J. Cheng, and P. C. K. Luk, "Analytical and experimental evaluation of SiC-inverter nonlinearities for traction drives used in electric vehicles," *IEEE Trans. Veh. Technol.*, vol. 67, no. 1, pp. 146–159, Jan. 2018.
- [5] X. Ding, M. Du, T. Zhou, H. Guo, and C. Zhang, "Comprehensive comparison between silicon carbide MOSFETs and silicon IGBTs based traction systems for electric vehicles," *Appl. Energy*, vol. 194, pp. 626–634, May 2017.
- [6] L. Yan, F. Wang, M. Dou, Z. Zhang, R. Kennel, and J. Rodriguez, "Active disturbance-rejection-based speed control in model predictive control for induction machines," *IEEE Trans. Ind. Electron.*, vol. 67, no. 4, pp. 2574–2584, Apr. 2020.
- [7] A. Andersson and T. Thiringer, "Assessment of an improved finite control set model predictive current controller for automotive propulsion applications," *IEEE Trans. Ind. Electron.*, vol. 67, no. 1, pp. 91–100, Jan. 2020.
- [8] L. Yan and F. Wang, "Observer-predictor-based predictive torque control of induction machine for robustness improvement," *IEEE Trans. Power Electron.*, vol. 36, no. 8, pp. 9477–9486, Aug. 2021.
- [9] L. Yan, F. Wang, P. Tao, and K. Zuo, "Robust predictive torque control of permanent magnet synchronous machine using discrete hybrid prediction model," *IEEE Trans. Energy Convers.*, vol. 35, no. 4, pp. 2240–2248, Dec. 2020.
- [10] B. Wang, Y. Yu, G. Wang, and D. Xu, "Static-errorless deadbeat predictive current control using second-order sliding-mode disturbance observer for induction machine drives," *IEEE Trans. Power Electron.*, vol. 33, no. 3, pp. 2395–2403, Mar. 2018.
- [11] X. Zhang, B. Hou, and Y. Mei, "Deadbeat predictive current control of permanent-magnet synchronous motors with stator current and disturbance observer," *IEEE Trans. Power Electron.*, vol. 32, no. 5, pp. 3818–3834, May 2017.
- [12] G. Pei, J. Liu, X. Gao, W. Tian, L. Li, and R. Kennel, "Deadbeat predictive current control for SPMSM at low switching frequency with moving horizon estimator," *IEEE J. Emerg. Sel. Topics Power Electron.*, vol. 9, no. 1, pp. 345–353, Feb. 2021.
- [13] Y. Yao, Y. Huang, F. Peng, J. Dong, and H. Zhang, "An improved dead-beat predictive current control with online parameter identification for surface-mounted PMSMs," *IEEE Trans. Ind. Electron.*, vol. 67, no. 12, pp. 10145–10155, Dec. 2019.
- [14] A. Brosch, S. Hanke, O. Wallscheid, and J. Bocker, "Data-driven recursive least squares estimation for model predictive current control of permanent magnet synchronous motors," *IEEE Trans. Power Electron.*, vol. 36, no. 2, pp. 2179–2190, Feb. 2021.

- [15] K. Zhang, M. Fan, Y. Yang, R. Chen, Z. Zhu, C. Garcia, and J. Rodriguez, "Tolerant sequential model predictive direct torque control of permanent magnet synchronous machine drives," *IEEE Trans. Transport. Electrification*, vol. 6, no. 3, pp. 1167–1176, Sep. 2020.
- [16] F. Wang, H. Xie, Q. Chen, S. A. Davari, J. Rodriguez, and R. Kennel, "Parallel predictive torque control for induction machines without weighting factors," *IEEE Trans. Power Electron.*, vol. 35, no. 2, pp. 1779–1788, Feb. 2020.
- [17] Y. Zhang, H. Yang, and B. Xia, "Model-predictive control of induction motor drives: Torque control versus flux control," *IEEE Trans. Ind. Appl.*, vol. 52, no. 5, pp. 4050–4060, Sep./Oct. 2016.
- [18] S. Huang, G. Wu, F. Rong, C. Zhang, S. Huang, and Q. Wu, "Novel predictive stator flux control techniques for PMSM drives," *IEEE Trans. Power Electron.*, vol. 34, no. 9, pp. 8916–8929, Sep. 2019.
- [19] M. Novak, H. Xie, T. Dragicevic, F. Wang, J. Rodriguez, and F. Blaabjerg, "Optimal cost function parameter design in predictive torque control (PTC) using artificial neural networks (ANN)," *IEEE Trans. Ind. Electron.*, vol. 68, no. 8, pp. 7309–7319, Aug. 2021.
- [20] S. A. Davari, V. Nekoukar, C. Garcia, and J. Rodriguez, "Online weighting factor optimization by simplified simulated annealing for finite set predictive control," *IEEE Trans. Ind. Informat.*, vol. 17, no. 1, pp. 31–40, Jan. 2021.
- [21] H. Fretes, J. Rodas, J. Doval-Gandoy, V. Gomez, N. Gomez, M. Novak, J. Rodriguez, and T. Dragicevic, "Pareto optimal weighting factor design of predictive current controller of a six-phase induction machine based on particle swarm optimization algorithm," *IEEE J. Emerg. Sel. Topics Power Electron.*, vol. 10, no. 1, pp. 207–219, Feb. 2022.
- [22] M. Siami, D. A. Khaburi, A. Abbaszadeh, and J. Rodríguez, "Robustness improvement of predictive current control using prediction error correction for permanent-magnet synchronous machines," *IEEE Trans. Ind. Electron.*, vol. 63, no. 6, pp. 3458–3466, Jun. 2016.
- [23] F. Wang, K. Zuo, P. Tao, and J. Rodriguez, "High performance model predictive control for PMSM by using stator current mathematical model self-regulation technique," *IEEE Trans. Power Electron.*, vol. 35, no. 12, pp. 13652–13662, Dec. 2020.



RONG FU was born in Shaanxi, China, in 1977. She received the B.S. degree in electrical engineering from the Baoji University of Arts and Sciences, Baoji, in 2000, and the M.S. degree in electric machine and electric apparatus and the Ph.D. degree in electrical engineering from Northwestern Polytechnical University, Xi'an, China, in 2007 and 2015, respectively.

She is currently with Weinan Normal University. Her research interest includes optimal design and high-performance control of permanent magnet synchronous motor for electric vehicle.

• • •